Chemosphere 184 (2017) 1071–1079

Contents lists available at ScienceDirect

Chemosphere

journal homepage: www.elsevier.com/locate/chemosphere

Organic matters removal from landfill leachate by immobilized *Phanerochaete chrysosporium* loaded with graphitic carbon nitride under visible light irradiation

Liang Hu [a, b], Yutang Liu [a, b], Guangming Zeng [a, b, *], Guiqiu Chen [a, b, **], Jia Wan [a, b], Yunxiong Zeng [c], Longlu Wang [c], Haipeng Wu [a, b], Piao Xu [a, b], Chen Zhang [a, b], Min Cheng [a, b], Tianjue Hu [a, b]

[a] College of Environmental Science and Engineering, Hunan University, Changsha, Hunan, 410082, PR China
[b] Key Laboratory of Environmental Biology and Pollution Control (Hunan University), Ministry of Education, Changsha, Hunan, 410082, PR China
[c] State Key Laboratory of Chemo/Biosensing and Chemometrics, Hunan University, Changsha, 410082, PR China

HIGHLIGHTS

- Immobilized *P. chrysosporium* loaded with photocatalyst g-C_3N_4 was perfectly fabricated.
- The typical absorption edge in visible light region for g-C_3N_4 was at about 460 nm.
- Immobilized *P. chrysosporium* provided a larger number of active reaction sites.
- The TOC removal efficiency reached 74.99% in 72 h under visible light irradiation.
- Immobilized *P. chrysosporium* could remove almost all organic compounds in leachate.

GRAPHICAL ABSTRACT

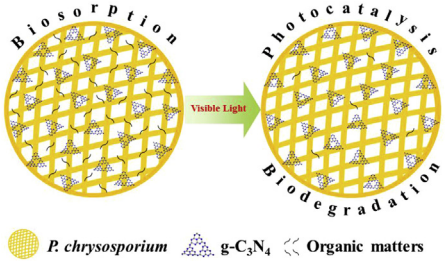

ARTICLE INFO

Article history:
Received 6 December 2016
Received in revised form
18 May 2017
Accepted 15 June 2017
Available online 16 June 2017

Handling Editor: Jun Huang

Keywords:
Graphitic carbon nitride
Landfill leachate
Organic matters removal
Photocatalytic degradation
Phanerochaete chrysosporium

ABSTRACT

This study investigated the technical applicability of a combination of *Phanerochaete chrysosporium* (*P. chrysosporium*) with photocatalyst graphitic carbon nitride (g-C_3N_4) for organic matters removal from landfill leachate under visible light irradiation. Photocatalyst g-C_3N_4 was well immobilized on the hyphae surface of *P. chrysosporium* by calcium alginate. The typical absorption edge in visible light region for g-C_3N_4 was at about 460 nm, and the optical absorption bandgap of g-C_3N_4 was estimated to be 2.70 eV, demonstrating the great photoresponsive ability of g-C_3N_4. An optimized g-C_3N_4 content of 0.10 g in immobilized *P. chrysosporium* and an optimized immobilized *P. chrysosporium* dosage of 1.0 g were suitable for organic matters removal. The removal efficiency of total organic carbon (TOC) reached 74.99% in 72 h with the initial TOC concentration of 100 mg L^{-1}. In addition, the gas chromatography coupled with mass spectrometry (GC-MS) measurements showed that immobilized *P. chrysosporium* presented an outstanding removal performance for almost all organic compounds in landfill leachate, especially for the volatile fatty acids and long-chain hydrocarbons. The overall results indicate that the combination

* Corresponding author. College of Environmental Science and Engineering, Hunan University, Changsha, 410082, PR China.
** Corresponding author. College of Environmental Science and Engineering, Hunan University, Changsha, Hunan, 410082, PR China.
E-mail addresses: zgming@hnu.edu.cn (G. Zeng), gqchen@hnu.edu.cn (G. Chen).

http://dx.doi.org/10.1016/j.chemosphere.2017.06.065

P. chrysosporium with photocatalyst g-C_3N_4 for organic matters removal from landfill leachate may provide a more comprehensive potential for the landfill leachate treatment.

1. Introduction

Sanitary landfill is one of the effective techniques for the treatment of municipal solid wastes. Landfill leachate belongs to complex wastewater, which is generated in the biodegradation process of solid wastes, including the inherent water of solid wastes itself and the rainwater as it permeates through solid wastes (Lei et al., 2007; Renou et al., 2008; Zhang et al., 2013). Due to the mixture of municipal solid wastes in landfill, the composition of landfill leachate contains a wide variety of harmful pollutants with respect to the climatic conditions, the landfill age, and the type of the deposited solid wastes (Vilar et al., 2011b). These harmful pollutants are usually classified into four groups: dissolved organic matters (DOMs, including recalcitrant compounds) (Kulikowska and Klimiuk, 2008; Cheng et al., 2016), inorganic macrocomponents (Zhang et al., 2013), heavy metals (including Cd, Cr, Hg, Cu, and Pb) (Fan et al., 2008; Feng et al., 2010; Vilar et al., 2011a), and xenobiotic organic compounds (such as dioxins and halogenated organics, etc.) (Zhang et al., 2007; Zhao et al., 2012). Since there is a possibility for landfill leachate to enter groundwater, many measures have been carried out in most of sanitary landfills to collect the leachate for treatment and minimize or prevent the permeation of leachate (Kurniawan et al., 2006; Zhao et al., 2012; Zeng et al., 2013a, 2013b).

Mature landfill leachate generally presents a low BOD_5/COD ratio (Vilar et al., 2011b), which indicates that the leachate contains high concentrations of ammonia nitrogen and recalcitrant organic compound. According to the characteristics of the mature leachate, the conventional treatment techniques, such as biological (anaerobic and aerobic methods) and physical/chemical (flocculation and flotation) processes, could not be effective enough to completely decline the negative impact of the leachate on environment (Renou et al., 2008; Silva et al., 2013; Ghazi et al., 2014; Sanchis et al., 2014). Therefore, the new-type treatment techniques have been widely investigated, including advanced oxidation processes (AOPs, the combination of super-strong oxidants, e.g. H_2O_2 or O_3 with high energy sources, e.g. ultrasound (US), electron beam (EB), ultraviolet (UV), catalysts (Fe^{2+}), and photocatalysts (TiO_2) to generate hydroxyl radicals (OH•)) (Kurniawan et al., 2006; Altin, 2008; Frontistis et al., 2008; Primo et al., 2008; Atmaca, 2009; Hermosilla et al., 2009), membrane filtration (e.g. reverse osmosis, microfiltration, ultrafiltration, and nanofiltration) (Ozturk et al., 2003; Pi et al., 2009; Barbosa et al., 2016), and adsorption (e.g. resins and activated carbon) (Rodrıguez et al., 2004; Rivas et al., 2006; Xu et al., 2012; Zhang et al., 2016). AOPs are usually considered to be the most superior methods for the landfill leachate treatment.

AOPs can be applied as the pre-treatment of biological process. Since it is able to improve the biodegradable ability of mature landfill leachate by generating the powerful OH•, which can degrade most recalcitrant organic molecules into a biodegradable intermedium, or even into H_2O and CO_2 (Barbosa et al., 2016). For example, photocatalysis has been widely used as the removal technique for recalcitrant organic pollutants such as benzene-based organics and organic dyes (Li et al., 2013). Wang et al. (2009) reported that graphitic carbon nitride (g-C_3N_4), as a promising metal-free polymeric photocatalyst, presented a great photocatalytic performance for the photodegradation of recalcitrant organic pollutants. Generally, g-C_3N_4 can be easily synthesized by a simple method such as direct calcination of carbamide, and it is composed of nitrogen, carbon, and a small amount of hydrogen (Pan et al., 2011; Du et al., 2012). What's more, g-C_3N_4 is highly stable with regard to light irradiation, chemical, and thermal because of the strong covalent bonds between nitrogen and carbon atom. Thus the nontoxic and reusable g-C_3N_4 is considered as a significant photocatalyst for practical application.

Additionally, fungal treatment for landfill leachate has also been widely investigated (Ellouze et al., 2008; Kalčíková et al., 2014; Hu et al., 2016). For example, white rot fungi have presented considerable potential for utilization in toxic and hazardous pollutants removal (Kalčíková et al., 2014; Hu et al., 2016). White rot fungi are able to secrete various extracellular enzymes (e.g. laccase (Lac), lignin peroxidase (LiP), and manganese peroxidase (MnP)), which are competent to the biodegradation of natural lignocellulosic substrates, and are also efficient in removing a wide range of organic pollutants such as phenols, dyes, pesticides, polychlorinated biphenyls, and so on (Huang et al., 2008; Brijwani et al., 2010). Our groups reported a successful application of white rot fungi for mature landfill leachate treatment (Hu et al., 2016). It is thought that extracellular enzymes produced by white rot fungi may be high efficiency in the whole process due to their ability in degrading macromolecule organic pollutants. Therefore, it is feasible and valuable to combine white rot fungi with photocatalyst g-C_3N_4 for organic matters removal from landfill leachate. To date, the correlative research has not been reported.

This study investigated the technical applicability of a combination of *Phanerochaete chrysosporium* (*P. chrysosporium*) with photocatalyst g-C_3N_4 for the organic matters removal from landfill leachate. *P. chrysosporium* and photocatalyst g-C_3N_4 were immobilized with calcium alginate to improve its mechanical strength and resistance to toxic organic pollutants. In addition, the effects of g-C_3N_4 content, initial total organic carbon (TOC) concentration, immobilized *P. chrysosporium* dosage, and lighting were investigated in details. The varieties of organic compounds in landfill leachate were also detected by gas chromatography coupled with mass spectrometry (GC-MS).

2. Materials and methods

2.1. Landfill leachate

The landfill leachate samples were collected from the refuse landfill of Heimifeng in Changsha, China. The samples were preserved with polyethylene bottles at a temperature of 4 °C. The TOC was analyzed with TOC ANALYZER (TOC-V_{CPH}, shimadzu). The ammonia nitrogen (NH_3-N), chemical oxygen demand (COD), and 5 d biochemical oxygen demand (BOD_5) were analyzed through standard methods (Apha, 1995). The final leachate samples were centrifuged at 10,000 rpm for 15 min using the superspeed refrigerated centrifuge and filtered using the 0.45 μm membranes to remove particles.

2.2. Microorganism and growth conditions

The *P. chrysosporium* BKM-F1767 (ATCC 24725) used in this work

was purchased from China Center for Type Culture Collection (Wuhan). The fungal spore was subcultured on potato dextrose agar slants using an inoculating loop, and then the potato dextrose agar slants were placed in constant humidity incubator at 37 °C for 5 d cultivation. The fungal mycelia suspensions were prepared through the dissolving fungal spores into sterile distilled water using a cotton swab under sterile condition, and the spore concentration was measured and adjusted to 1.0×10^6 CFU mL^{-1} using a turbidimeter (WGZ-200, Shanghai, China). The inoculum of fungal spores was obtained by adding 3 mL of the above spore suspensions to 100 mL of the Kirk's liquid culture medium (Kirk et al., 1978) in a 250 mL Erlenmeyer flask. Flasks were maintained at 37 °C in an orbital shaker under 150 rpm for 3 d.

2.3. Synthesis of graphitic carbon nitride

Photocatalyst g-C_3N_4 was synthesized using carbamide (Analytical Reagent, Sinopharm Chemical Reagent Beijing). 10 g carbamide was put in a lidded high quality alumina crucible, and the alumina crucible was wrapped with tinfoil to avoid volatilization during the heating process, and then placed inside a muffle furnace. The temperature was raised to 600 °C at a ramp rate of 5 °C min^{-1} and kept for 2 h to complete the reaction. The yellow powder product was washed three times with nitric acid (0.1 M) and distilled water, and then dried at 80 °C for 24 h (Wang et al., 2009).

2.4. Preparation of immobilized P. chrysosporium

P. chrysosporium was immobilized through mixing 100 mL *P. chrysosporium* spore suspension (1.0×10^6 CFU mL^{-1}), 100 mL sodium alginate solution (4%), and 0.1 g g-C_3N_4. The above mixture was injected dropwise into 200 mL sterile $CaCl_2$ solution (2%) using an injector to form globules, and the globules were hardened in the $CaCl_2$ solution for 3 h to improve their mechanical stability. Then, the globules were washed and transferred into the Kirk's liquid culture medium. After 3 d' cultivation in an orbital shaker (150 rpm) at 37 °C, the immobilized *P. chrysosporium* were rinsed with distilled water for use (Hu et al., 2016). All the operations were completed under sterile condition.

2.5. Characterizations of graphitic carbon nitride and immobilized P. chrysosporium

The morphologies and chemical compositions of g-C_3N_4 were performed using scanning electron microscope (SEM) (FEI QUANTA 200), transmittance electron microscopy (TEM) (JEOL, JEM-2100F), UV–vis diffuse reflectance spectrophotometer (DRS) (Agilent, Cary 300), X-ray diffraction (XRD) (D8-Advance, Bruker Company, Germany), fourier transform infrared (FTIR) spectrophotometer (WQF-410, China), and photoluminescence (PL) spectrophotometer (Hitachi F-7000). Environmental scanning electron microscope (ESEM) (FEI QUANTA 200) images of immobilized *P. chrysosporium* were obtained before and after the experiment to confirm the morphological changes of the mycelium. The elemental composition was obtained by using energy disperse spectroscopy (EDS) analyzer (FEI QUANTA 200) after gold plating at an acceleration voltage of 20 kV. Samples pretreatment were as follows: immobilized *P. chrysosporium* were filtered through a qualitative filter paper from aqueous solution and freezed in a refrigerator at −20 °C, and then dried in a vacuum freezing drying oven at −50 °C.

2.6. Organic matters removal experiments

2.6.1. Content of graphitic carbon nitride

The initial content of g-C_3N_4 in immobilized *P. chrysosporium* was adjusted to the various values, such as 0.06, 0.08, 0.10, 0.12, and 0.14 g. 100 mL landfill leachate with initial TOC concentration of 100 mg L^{-1} was added to 250 mL Erlenmeyer flask. The pH value of the solution was adjusted to 6.0 with 0.1 M HCl or 0.1 M NaOH. And all Erlenmeyer flasks were sterilized under 121 °C for 20 min. After sterilization, 1.0 g immobilized *P. chrysosporium* containing different contents of g-C_3N_4 were added to the above aqueous solutions which were agitated in an orbital shaker under 150 rpm with lighting (400–700 nm and 1000 Lux) at 37 °C. Afterwards, 2 mL samples were taken out by pipette from Erlenmeyer flasks at the setting time interval to detect the residual TOC concentrations.

2.6.2. Initial TOC concentration

A series of 100 mL landfill leachate with initial TOC concentrations of 50, 100, 150, and 200 mg L^{-1} were added to 250 mL Erlenmeyer flasks. The pH values of the solutions were adjusted to 6.0. After sterilization, 1.0 g immobilized *P. chrysosporium* containing 0.10 g g-C_3N_4 were added to the above aqueous solutions which were agitated in an orbital shaker under 150 rpm with lighting (400–700 nm and 1000 Lux) at 37 °C. The batch experiments were carried out by g-C_3N_4, immobilized g-C_3N_4, *P. chrysosporium*, immobilized *P. chrysosporium* without g-C_3N_4, and immobilized *P. chrysosporium* with g-C_3N_4, respectively. The initial TOC concentration was 100 mg L^{-1}, the individual g-C_3N_4 weight was 0.10 g, the individual *P. chrysosporium* weight was 0.90 g, and the individual immobilized *P. chrysosporium* with g-C_3N_4 weight was 1.0 g. All Erlenmeyer flasks containing 100 mL landfill leachate were sterilized and adjusted to pH of 6.0 in an orbital shaker with the condition mentioned above.

2.6.3. Dosage of immobilized P. chrysosporium

The initial dosage of immobilized *P. chrysosporium* containing 0.10 g g-C_3N_4 was adjusted to the various values, such as 0.5, 1.0, 1.5, 2.0, and 2.5 g. The initial TOC concentration of landfill leachate was 100 mg L^{-1}, and all Erlenmeyer flasks containing 100 mL aqueous solution were sterilized and adjusted to pH of 6.0 in an orbital shaker with the condition mentioned above.

2.6.4. Effect of lighting

100 mL landfill leachate with initial TOC concentration of 100 mg L^{-1} was added to 250 mL Erlenmeyer flask, then sterilized and adjusted to pH of 6.0. 1.0 g immobilized *P. chrysosporium* containing 0.10 g g-C_3N_4 was added to the above aqueous solutions which were agitated in an orbital shaker under 150 rpm at 37 °C with or without lighting (400–700 nm and 1000 Lux).

2.7. GC-MS analysis

The landfill leachate samples were extracted with dichloromethane (HPLC grade). 20 mL of the sample was initially extracted with 10 mL of dichloromethane under neutral condition, then in acidic condition by adding drops of H_2SO_4 solution, then in alkaline condition by adding drops of NaOH solution using separating funnel. Each extraction was operated twice. Finally, the combined extraction (about 60 mL) was dehydrated with anhydrous Na_2SO_4 and concentrated at 50 °C by a rotary evaporation (Lei et al., 2007).

1 μL extracted sample was measured by a GC-MS spectrometer (Model QP-2010, Shimadzu, Japan), equipped with a Rtx-50 capillary chromatographic column (30 m × 0.25 mm, 0.25 μm film thickness). The flow rate of the carrier gas (highly pure He) was 50 cm s^{-1}. After beginning under isothermal conditions at 65 °C (held for 2 min), the temperature was raised to 220 °C at a rate of 9 °C min^{-1} and held for 20 min. The injector and transfer-line temperature was 300 °C. The electron impact of MS was applied as an ionization technique at 70 eV, scan field 35–350 *m/z*, the split

ratio was 1: 10, injector port and ion source temperatures were 170 °C and 200 °C, respectively.

3. Results and discussion

3.1. Characteristics of landfill leachate

Table S1 presented the main physicochemical characteristics of the raw landfill leachate used in this work. The raw landfill leachate displayed a strong malodorous black, which was related to high organic matters content (COD = 6250 mg L^{-1}, BOD_5 = 630 mg L^{-1}, TOC = 1920 mg L^{-1}) and high ammonia nitrogen charge (NH_3-N = 2045 mg L^{-1}). A low BOD_5/COD (0.10) ratio indicated the low biodegradability of the raw landfill leachate, which could be affirmed as the mature landfill leachate. The pH value was 8.02, presenting alkalescency, which was associated with high ammonia nitrogen charge. There was also a high concentration of potassium (1.83 g L^{-1}) and sodium (2.31 g L^{-1}) within the leachate, which resulted in a high conductivity of 20.3 mS cm^{-1}. In addition, the concentrations of iron and manganese were more relative high than that of heavy metals, and the raw leachate contained a relatively low content of heavy metals except lead.

3.2. Characterizations of graphitic carbon nitride and immobilized P. chrysosporium

3.2.1. Scanning electron microscopy and transmittance electron microscopy analysis

The structural and morphological characteristic of g-C_3N_4 synthesized from the pyrolysis of carbamide under ambient pressure at 600 °C was observed using SEM and TEM. From Fig. 1a, it could be seen that the g-C_3N_4 powder presented obvious irregular folding structures and two dimensional lamellar structures with wrinkles. After ultrasonic treatment of 3 h for g-C_3N_4 sample, it could be clearly seen that the g-C_3N_4 powder showed obvious mesoporous sheet structure from Fig. 1b. These structural characteristics of g-C_3N_4 were favorable for the photo-induced charge transfer and then provided a good basis for the photocatalysis reaction (Chen et al., 2014).

The morphologies of immobilized *P. chrysosporium* were investigated by ESEM. Fig. 1c showed that the hyphae of *P. chrysosporium* were not only grew on the surface of immobilized *P. chrysosporium*, but also in the interspaces, thereby presenting a spatial retiform structure. ESEM images indicated that the immobilized *P. chrysosporium* contained a great amount of tiny interspaces that could provide a larger number of adsorptive sites for the pollutants (Hu et al., 2016). And g-C_3N_4 particles were well fixed on *P. chrysosporium* by calcium alginate. From Fig. 1d–f, it could be also found that the hyphae of immobilized *P. chrysosporium* were loosely assembled, and they became more gracile after reaction with the increase of initial TOC concentration, indicating that landfill leachate was poisonous to the immobilized *P. chrysosporium* to some extent (Hu et al., 2016). The variety of elements in the immobilized *P. chrysosporium* was analyzed by EDS (Fig. S1).

3.2.2. X-ray diffraction, UV–vis diffuse reflectance spectrophotometer and photoluminescence spectrum analysis

Fig. 2a showed XRD pattern of g-C_3N_4 composition. Two obvious peaks were found in g-C_3N_4 at around 27.5° (002) and 13.1° (100), which could be indicative of the characteristic inter-planar stacking and in-planar repeating unit peaks of the aromatic series in graphite-like carbon nitride (Liu et al., 2011). Fig. 2b depicted the UV–vis absorbance spectrum and Kubelka-Munk transformed reflectance spectrum of g-C_3N_4. It could be seen from Fig. 2b that the UV–vis absorbance spectrum of g-C_3N_4 presented typical semiconductor optical characteristics. The typical absorption edge in visible light region for g-C_3N_4 was at about 460 nm, which demonstrated that the g-C_3N_4 could absorb solar light with wavelength shorter than 460 nm (Bai et al., 2014; Chen et al., 2014). The Kubelka-Munk transformed reflectance spectrum showed that the optical absorption bandgap of g-C_3N_4 was estimated to be 2.70 eV (Kumar et al., 1999). Based on above analysis, the g-C_3N_4 synthesized from the pyrolysis of carbamide under ambient pressure at 600 °C could contribute to the great photoresponsive ability. To explore the trapping and transfer property of electron-hole pairs, PL spectrum of g-C_3N_4 was recorded. From Fig. 2c, it could be found that the g-C_3N_4 presented the strongest emission peak at about 463 nm at ambient temperature, which came up to the bandgap energy of 2.70 eV (Zhou et al., 2014).

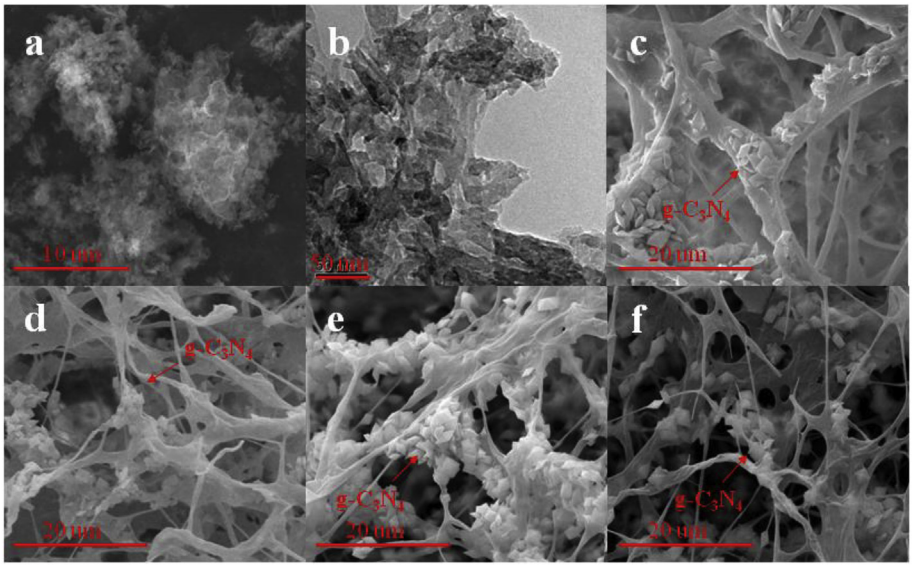

Fig. 1. SEM (a) and TEM (b) images of g-C_3N_4. ESEM images of immobilized *P. chrysosporium*. (c) in native form, (d) 1 g after reaction with 100 mg L^{-1} of landfill leachate, (e) 2 g after reaction with 50 mg L^{-1} of landfill leachate, (f) 2 g after reaction with 100 mg L^{-1} of landfill leachate, respectively.

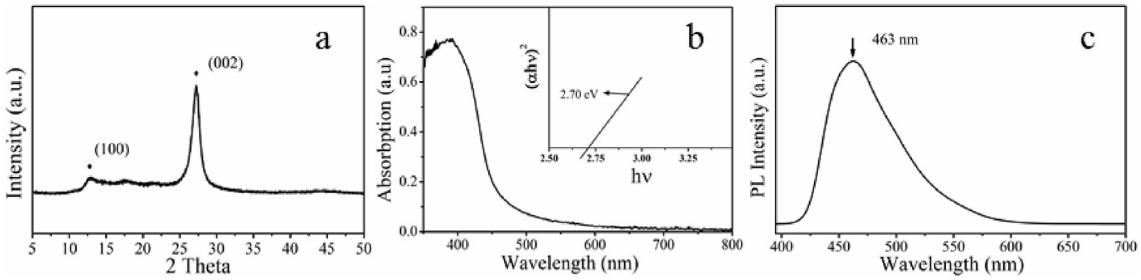

Fig. 2. XRD pattern (a), UV–vis absorbance spectrum (b), Photoluminescence spectrum (c) of g-C_3N_4, respectively.

3.2.3. Fourier transform infrared spectrophotometer analysis

Fig. 3 depicted the FTIR spectra of immobilized *P. chrysosporium*, *P. chrysosporium*, and g-C_3N_4. The changes in the surface characteristics and the functional groups of hyphae were analyzed before and after immobilization. Compared with Fig. 3a and b, FTIR spectra of immobilized *P. chrysosporium* and *P. chrysosporium* demonstrated that the existence of different characteristic peaks was in agreement with the possible existence of carboxylic, hydroxyl, and amino groups on the hyphae surface. The strong broad O-H stretching and the -NH groups stretching of carboxylic bounds in the region of 3436 cm^{-1} were obviously seen. The antisymmetric vibration of -CH_2 groups by the stretching of -OH groups could be responsible to the peak appearing at 2932 cm^{-1}. The peaks observed in the region of 1643 cm^{-1} were the characteristic of C=O groups stretching from aldehydes and ketones. In addition, the peaks at 1415 and 1329 cm^{-1} represented C-H binds and -CH_3 wagging in the carboxylic acid, respectively. The peak at 1235 cm^{-1} represented C-N heterocycle of g-C_3N_4, and the peak at 1047 cm^{-1} represented C-N stretching of aliphatic amines (Hu et al., 2016). From Fig. 3c, the absorption peak at 1647 cm^{-1} could be assigned to the C-N stretching vibration, while the four strong absorption peak in the region of 1556, 1410, 1319, and 1230 cm^{-1} corresponded to the typical stretching of C-N heterocycles (Yan et al., 2009), the absorption peak observed at 801 cm^{-1} could be ascribed to the out-of-plane ring bending of C-N heterocycles (Zhang et al., 2008; Wang et al., 2011). Based on above analysis, it indicated that *P. chrysosporium* and g-C_3N_4 were successfully immobilized by calcium alginate.

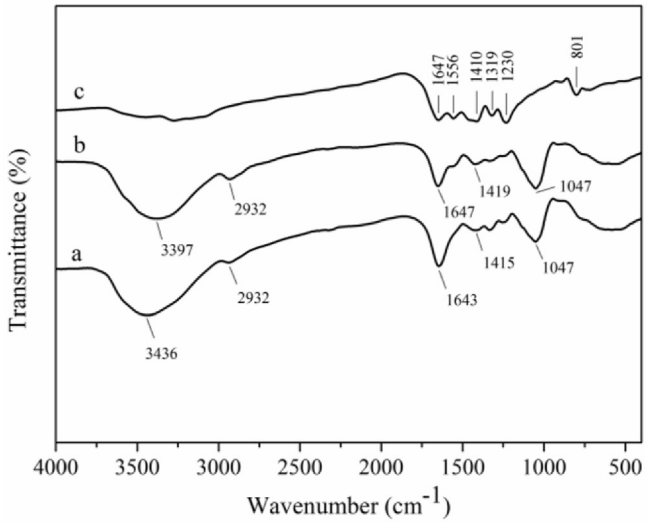

Fig. 3. FTIR spectra for (a) immobilized *P. chrysosporium*, (b) *P. chrysosporium*, (c) g-C_3N_4 in the region between 4000 and 400 cm^{-1}, respectively.

3.3. Organic matters removal by immobilized P. chrysosporium

3.3.1. Content of graphitic carbon nitride

An optimized g-C_3N_4 content in immobilized *P. chrysosporium* was essentially demanded to maximize the efficiency of photocatalytic degradation. As shown in Fig. 4, the removal efficiency of organic matters was sensitive to the variation of g-C_3N_4 content in immobilized *P. chrysosporium*. With an increasing initial g-C_3N_4 content of 0.06, 0.08, 0.10, 0.12, and 0.14 g, the TOC residual concentration reached 77.25, 46.99, 25.01, 37.10, and 60.21 mg L^{-1}, respectively, and the TOC removal efficiency were 22.75%, 53.01%, 74.99%, 62.90%, and 39.79%, respectively. A transparent trend was found, the TOC removal efficiency firstly increased from 22.75% to 74.99% when the g-C_3N_4 content increasing from 0.06 g to 0.10 g, then the TOC removal efficiency gradually decreased from 74.99% to 39.79% when the g-C_3N_4 content increasing from 0.10 g to 0.14 g, indicating an optimized g-C_3N_4 content (0.10 g) in immobilized *P. chrysosporium* existed in the photocatalytic degradation process. Because the increase of g-C_3N_4 content could promote the use ratio of light energy to some extent, while the excessive g-C_3N_4 might cause more stacking of the reaction system, leading to an undesirable light penetration through the landfill leachate (Chen et al., 2016).

3.3.2. Effect of initial TOC concentration

As shown in Fig. 5A, it could be seen that with an increasing initial TOC concentration of 50, 100, 150, and 200 mg L^{-1}, the TOC residual concentration reached 10.21, 25.01, 65.15, and

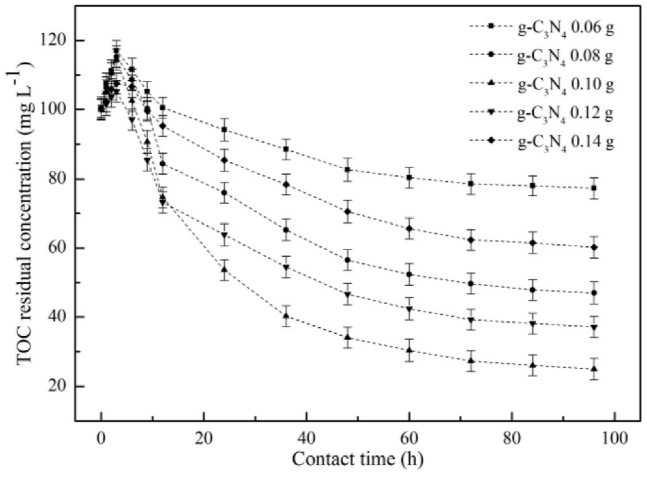

Fig. 4. Effect of g-C_3N_4 content on organic matters removal from landfill leachate using immobilized *P. chrysosporium* under lighting. Initial TOC concentration was 100 mg L^{-1} and immobilized *P. chrysosporium* dosage was 1.0 g, respectively. The *bars* represented the standard deviations (SD) of means (n = 3).

132.24 mg L^{-1}, respectively, and the TOC removal efficiency were 79.58%, 74.99%, 56.57%, and 33.88%, respectively. It was evident that the initial TOC concentration played a significant role in photocatalysis and biodegradation process. The TOC concentration was observed to increase considerably in the period from 0 h to 3 h. This was mainly attributed to the extracellular enzymes secreted by immobilized *P. chrysosporium*, such as MnP and LiP, leading to the growth of TOC concentration (Huang et al., 2008; Yang et al., 2010). After this period, a rapidly declining tendency appeared with an increase in contact time from 3 h to 36 h. There were three reasons for the decrease of TOC residual concentration. As follow: (1) The immobilized *P. chrysosporium* contained a great amount of tiny interspaces that could provide a larger number of adsorptive sites for the dissolved organic matters; (2) The dissolved organic matters adsorbed on the hyphae surface were degraded by the photocatalysis of g-C_3N_4, and this step provided a convenience for the biodegradation; (3) The dissolved organic matters were biodegraded by the extracellular enzymes (MnP and LiP) secreted from immobilized *P. chrysosporium* (Kalčíková et al., 2014). After 60 h, the TOC residual concentration did not mainly change with the further increase in contact time, suggesting that the adsorption and degradation reaction reached equilibrium.

In order to confirm the synergetic effect of *P. chrysosporium* and g-C_3N_4 for TOC removal, the batch experiments were investigated at initial TOC concentration of 100 mg L^{-1} with lighting by g-C_3N_4, immobilized g-C_3N_4, *P. chrysosporium*, immobilized *P. chrysosporium* without g-C_3N_4, and immobilized *P. chrysosporium* with g-C_3N_4, respectively. As shown in Fig. 5B, the maximum removal efficiency of TOC reached 74.99% when using immobilized *P. chrysosporium* with g-C_3N_4, while immobilized *P. chrysosporium* without g-C_3N_4, *P. chrysosporium*, immobilized g-C_3N_4, and g-C_3N_4 only reached 44.83%, 39.98%, 21.44%, and 24.95%, respectively. The removal efficiency of TOC by immobilized *P. chrysosporium* with g-C_3N_4 increased by 69% and 250% compared to those of immobilized *P. chrysosporium* without g-C_3N_4 and immobilized g-C_3N_4, respectively. The result could be attributed to the synergetic effect of *P. chrysosporium* and g-C_3N_4. However, the maximum removal efficiency of TOC by immobilized *P. chrysosporium* with g-C_3N_4, immobilized *P. chrysosporium* without g-C_3N_4, *P. chrysosporium*, immobilized g-C_3N_4, and g-C_3N_4 without lighting only reached 32.18%, 42.01%, 40.77%, 5.74%, and 5.36%, respectively. This result further implied that g-C_3N_4 loaded on the hyphae played a key role in the improvement of photocatalysis ability for immobilized *P. chrysosporium*, and the removal ability of immobilized *P. chrysosporium* with g-C_3N_4 was also improved to a great extent under lighting. In this aspect, the spatial retiform structure of immobilized *P. chrysosporium* allowed the organic matters in leachate to diffuse into its interior space and to make contact with g-C_3N_4 loaded on the hyphae surface. Then some refractory organic matters could be degraded due to the photocatalysis of g-C_3N_4, which led to the highest removal efficiency of immobilized *P. chrysosporium*. Meanwhile, the mechanical strength of immobilized *P. chrysosporium* was enormously enhanced by calcium alginate, thereby avoiding rupture and diffusion problems (Couto, 2009). In addition, the recycling experiment results were shown in Fig. S2. After three cycles, the removal efficiency of TOC by immobilized *P. chrysosporium* only reached 7.35%, which reduced by 90.20% compared to that of the first cycle. The result may attribute to the short lifecycle of immobilized *P. chrysosporium*.

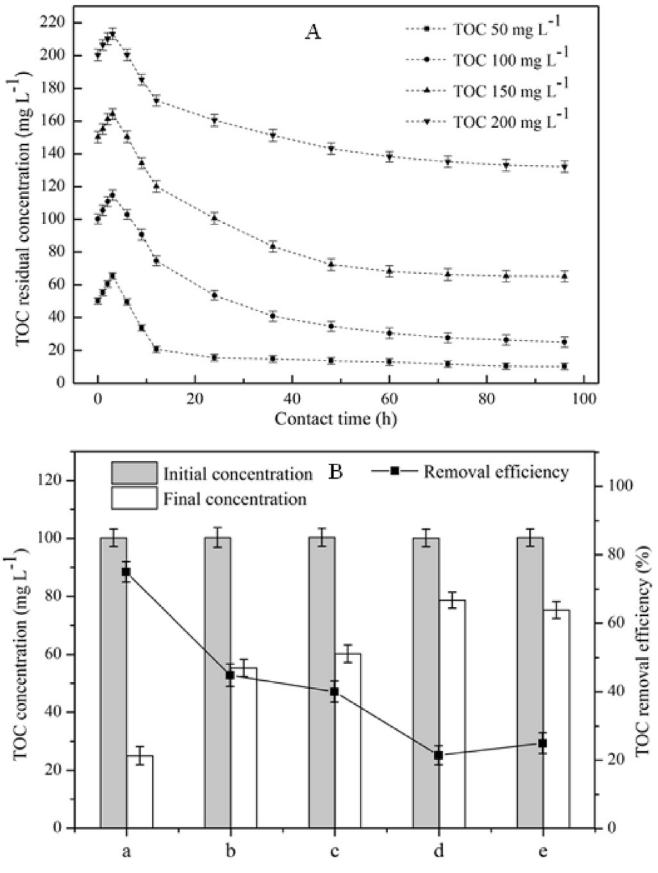

Fig. 5. (A) Effect of initial TOC concentration on organic matters removal from landfill leachate using immobilized *P. chrysosporium* with g-C_3N_4 under lighting. (B) Organic matters removal from landfill leachate using (a) immobilized *P. chrysosporium* with g-C_3N_4, (b) immobilized *P. chrysosporium* without g-C_3N_4, (c) *P. chrysosporium*, (d) immobilized g-C_3N_4, (e) g-C_3N_4 under lighting, respectively. The *bars* represented the standard deviations (SD) of means (n = 3).

3.3.3. Dosage of immobilized P. chrysosporium

An optimized immobilized *P. chrysosporium* dosage was essentially established to maximize the interactions between organic matters and reaction sites on the hyphae surface of immobilized *P. chrysosporium* (Gong et al., 2009; Hu et al., 2011). As could be observed from Fig. 6, the removal efficiency and equilibrium capacity of organic matters were greatly sensitive to the variation of the immobilized *P. chrysosporium* dosages. The TOC removal efficiency firstly increased from 44.75% to 74.99% when the immobilized *P. chrysosporium* dosage adding from 0.5 g to 1.0 g. This occurred because the increasing dosage of immobilized

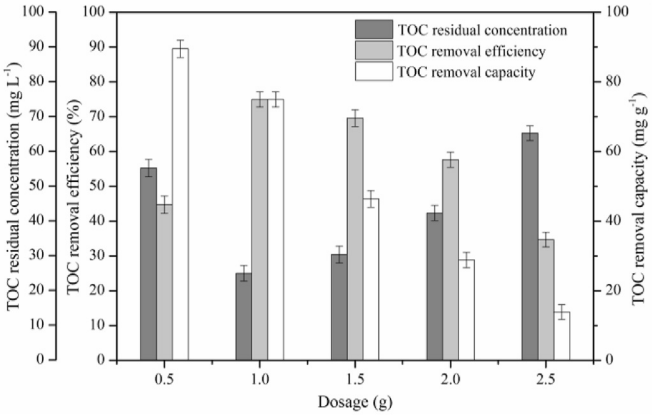

Fig. 6. Effect of immobilized *P. chrysosporium* dosage on organic matters removal from landfill leachate using immobilized *P. chrysosporium* under lighting. g-C_3N_4 content in immobilized *P. chrysosporium* was 0.10 g and initial TOC concentration was 100 mg L^{-1}, respectively. The *bars* represented the standard deviations (SD) of means (n = 3).

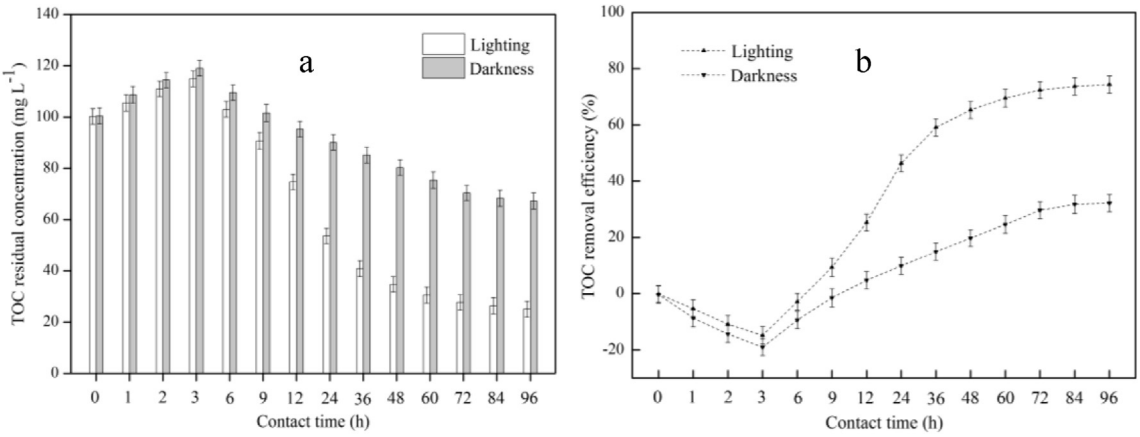

Fig. 7. Effect of lighting on organic matters removal from landfill leachate using immobilized *P. chrysosporium*. (a) TOC residual concentration, (b) TOC removal efficiency. g-C_3N_4 content in immobilized *P. chrysosporium* was 0.10 g; initial TOC concentration was 100 mg L^{-1}; and immobilized *P. chrysosporium* dosage was 1.0 g, respectively. The *bars* represented the standard deviations (SD) of means (n = 3).

P. chrysosporium increased the reaction sites on the hyphae surface and the density of the getatable reactive groups for organic matters, resulting in a higher removal efficiency of TOC. But the subsequent addition of immobilized *P. chrysosporium* from 1.0 g to 2.5 g showed a decreasing removal efficiency from 74.99% to 34.70%, which could be attributed to the partial aggregation of immobilized *P. chrysosporium* (Gupta et al., 2010) and the declining utilization rate of optical energy for photocatalytic degradation. However, the TOC removal capacity gradually decreased from 89.49 mg g^{-1} to 13.89 mg g^{-1} with the increasing dosage of immobilized *P. chrysosporium* from 0.5 g to 2.5 g. This was ascribed to the overcrowding of immobilized *P. chrysosporium*, which was a consequence of the overlapping reaction sites, leading to reduce in the available reaction sites and the overall surface area of immobilized *P. chrysosporium* (Lata et al., 2008; Chen et al., 2011). Therefore, these results indicated that an optimized immobilized *P. chrysosporium* dosage (1.0 g) existed in the removal procedure of organic matters from landfill leachate.

3.3.4. Effect of lighting

As described in Fig. 7, it could be perceived that the lighting had a significant influence on immobilized *P. chrysosporium* for organic matters removal from landfill leachate, and the photocatalysis of g-C_3N_4 loaded on the hyphae surface played a vital role in this procedure. From Fig. 7a, there was a fractional loss in the TOC concentration from 100.41 mg L^{-1} to 67.22 mg L^{-1} after 96 h treatment in the darkness, verifying the weak biosorption and biodegradation ability of immobilized *P. chrysosporium* for organic matters (Tang et al., 2008; Kalčíková et al., 2014). But the TOC removal ability of immobilized *P. chrysosporium* was greatly improved with the introduction of lighting by combining the photocatalytic degradation of g-C_3N_4 and the biosorption and biodegradation of *P. chrysosporium*. Thus the TOC concentration sharply declined to 25.01 mg L^{-1} after 96 h treatment in the lighting. Fig. 7b showed that the TOC removal efficiency finally reached 74.99% and 32.18% in the lighting and the darkness, respectively.

3.4. Organic compounds analysis

From Table S2, the species and peak area percentage of organic compounds in the original leachate decreased sharply after treatment with immobilized *P. chrysosporium*, presenting an outstanding removal performance for almost all organic compounds in landfill leachate, especially for the volatile fatty acids and long-chain hydrocarbons such as cyclohexylmethyl octadecyl ester, tetrapentacontane, bisnorhopane, heneicosane, tetracosane, hexatriacontane, and tetracontane, etc. It could be clearly observed that there were 30 kinds of organic compounds detected by GC-MS in the original landfill leachate, and almost 26 kinds of organic compounds were absolutely removed by immobilized *P. chrysosporium* in 36 h. There were also four new organic compounds in the process, which were speculated as the intermediate. After 72 h, all organic compounds in landfill leachate were completely removed (except for non-detected). Based on above results, the organic matters removal from landfill leachate with immobilized *P. chrysosporium* could be superior to one using the conventional biological method. As shown in Fig. S3, it was evident that the organic compounds in landfill leachate were mainly removed by immobilized *P. chrysosporium* under visible light irradiation. In addition, the landfill leachate samples treated by immobilized *P. chrysosporium* still contained some non-degradable DOMs such as fulvic acids and humic acids, which were hardly detected by GC-MS (Lei et al., 2007).

4. Conclusions

In this study, immobilized *P. chrysosporium* loaded with g-C_3N_4 was perfectly fabricated for the organic matters removal from landfill leachate under visible light irradiation. For the immobilized *P. chrysosporium*, the spatial retiform structure contained a great number of tiny interspaces, which provided a larger number of active reaction sites for the organic matters. An optimized g-C_3N_4 content of 0.10 g in immobilized *P. chrysosporium* and an optimized immobilized *P. chrysosporium* dosage of 1.0 g were suitable for organic matters removal. The TOC removal efficiency reached 74.99% in 72 h with the initial TOC concentration of 100 mg L^{-1}. Meanwhile, the ability of immobilized *P. chrysosporium* to remove organic matters from landfill leachate was higher than that of *P. chrysosporium* and g-C_3N_4. In addition, immobilized *P. chrysosporium* presented an outstanding removal performance for almost all organic compounds in landfill leachate, especially for the volatile fatty acids and long-chain hydrocarbons. Therefore, new insight into the combination *P. chrysosporium* with photocatalyst g-C_3N_4 for organic matters removal may provide a more comprehensive potential for the landfill leachate treatment.

Acknowledgments

This work was financially supported by the National Natural

Science Foundation of China (51521006, 51378190, 51378187, and 51579099), the Environmental Protection Technology Research Program of Hunan (2007185), the Program for Changjiang Scholars and Innovative Research Team in University (IRT-13R17) and Hunan Provincial Natural Science Foundation of China (2015JJ2031).

Appendix A. Supplementary data

Supplementary data related to this article can be found at http://dx.doi.org/10.1016/j.chemosphere.2017.06.065.

References

Altin, A., 2008. An alternative type of photoelectro-Fenton process for the treatment of landfill leachate. Sep. Purif. Technol. 61, 391–397.
Apha, A., WPCF, 1995. Standard Methods for the Examination of Water and Wastewater. American Public Health Association, Washington, DC, p. 456.
Atmaca, E., 2009. Treatment of landfill leachate by using electro-Fenton method. J. Hazard. Mater 163, 109–114.
Bai, X., Wang, L., Wang, Y., Yao, W., Zhu, Y., 2014. Enhanced oxidation ability of g-C3N4 photocatalyst via C60 modification. Appl. Catal. B Environ. 152, 262–270.
Barbosa, M.O., Moreira, N.F., Ribeiro, A.R., Pereira, M.F., Silva, A.M., 2016. Occurrence and removal of organic micropollutants: an overview of the watch list of EU Decision 2015/495. Water Res. 94, 257–279.
Brijwani, K., Rigdon, A., Vadlani, P.V., 2010. Fungal laccases: production, function, and applications in food processing. Enzyme Res. 2010.
Chen, A., Zeng, G., Chen, G., Fan, J., Zou, Z., Li, H., Hu, X., Long, F., 2011. Simultaneous cadmium removal and 2, 4-dichlorophenol degradation from aqueous solutions by *Phanerochaete chrysosporium*. Appl. Microbiol. Biot. 91, 811–821.
Chen, F., Yang, Q., Zhong, Y., An, H., Zhao, J., Xie, T., Xu, Q., Li, X., Wang, D., Zeng, G., 2016. Photo-reduction of bromate in drinking water by metallic Ag and reduced graphene oxide (RGO) jointly modified $BiVO_4$ under visible light irradiation. Water Res. 101, 555–563.
Chen, J., Shen, S., Guo, P., Wang, M., Wu, P., Wang, X., Guo, L., 2014. In-situ reduction synthesis of nano-sized Cu2O particles modifying g-C3N4 for enhanced photocatalytic hydrogen production. Appl. Catal. B Environ. 152–153, 335–341.
Cheng, Y., He, H., Yang, C., Zeng, G., Li, X., Chen, H., Yu, G., 2016. Challenges and solutions for biofiltration of hydrophobic volatile organic compounds. Biotechnol. Adv. 34, 1091–1102.
Couto, S.R., 2009. Dye removal by immobilised fungi. Biotechnol. Adv. 27, 227–235.
Du, A., Sanvito, S., Li, Z., Wang, D., Jiao, Y., Liao, T., Sun, Q., Ng, Y.H., Zhu, Z., Amal, R., 2012. Hybrid graphene and graphitic carbon nitride nanocomposite: gap opening, electron–hole puddle, interfacial charge transfer, and enhanced visible light response. J. Am. Chem. Soc. 134, 4393–4397.
Ellouze, M., Aloui, F., Sayadi, S., 2008. Detoxification of Tunisian landfill leachates by selected fungi. J. Hazard. Mater 150, 642–648.
Fan, T., Liu, Y., Feng, B., Zeng, G., Yang, C., Zhou, M., Zhou, H., Tan, Z., Wang, X., 2008. Biosorption of cadmium (II), zinc (II) and lead (II) by *Penicillium simplicissimum*: isotherms, kinetics and thermodynamics. J. Hazard. Mater 160, 655–661.
Feng, Y., Gong, J.L., Zeng, G.M., Niu, Q.Y., Zhang, H.Y., Niu, C.G., Deng, J.H., Yan, M., 2010. Adsorption of Cd (II) and Zn (II) from aqueous solutions using magnetic hydroxyapatite nanoparticles as adsorbents. Chem. Eng. J. 162, 487–494.
Frontistis, Z., Xekoukoulotakis, N.P., Diamadopoulos, E., Mantzavinos, D., 2008. Ozonation of landfill leachates: treatment optimization by factorial design. J. Adv. Oxid. Technol. 11, 370–376.
Ghazi, N.M., Lastra, A.A., Watts, M.J., 2014. Hydroxyl radical (OH) scavenging in young and mature landfill leachates. Water Res. 56, 148–155.
Gong, J.L., Wang, B., Zeng, G.M., Yang, C.P., Niu, C.G., Niu, Q.Y., Zhou, W.J., Liang, Y., 2009. Removal of cationic dyes from aqueous solution using magnetic multi-wall carbon nanotube nanocomposite as adsorbent. J. Hazard. Mater 164, 1517–1522.
Gupta, V.K., Rastogi, A., Nayak, A., 2010. Biosorption of nickel onto treated alga (*Oedogonium hatei*): application of isotherm and kinetic models. J. Colloid. Interf. Sci. 342, 533–539.
Hermosilla, D., Cortijo, M., Huang, C.P., 2009. Optimizing the treatment of landfill leachate by conventional Fenton and photo-Fenton processes. Sci. Total Environ. 407, 3473–3481.
Hu, L., Zeng, G., Chen, G., Dong, H., Liu, Y., Wan, J., Chen, A., Guo, Z., Yan, M., Wu, H., 2016. Treatment of landfill leachate using immobilized *Phanerochaete chrysosporium* loaded with nitrogen-doped TiO_2 nanoparticles. J. Hazard. Mater 301, 106–118.
Hu, X.J., Wang, J.S., Liu, Y.G., Li, X., Zeng, G.M., Bao, Z.L., Zeng, X.X., Chen, A.W., Long, F., 2011. Adsorption of chromium (VI) by ethylenediamine-modified cross-linked magnetic chitosan resin: isotherms, kinetics and thermodynamics. J. Hazard. Mater 185, 306–314.
Huang, D.L., Zeng, G.M., Feng, C.L., Hu, S., Jiang, X.Y., Tang, L., Su, F.F., Zhang, Y., Zeng, W., Liu, H.L., 2008. Degradation of lead-contaminated lignocellulosic waste by *Phanerochaete chrysosporium* and the reduction of lead toxicity. Environ. Sci. Technol. 42, 4946–4951.
Kalčíková, G., Babič, J., Pavko, A., Gotvajn, A.Ž., 2014. Fungal and enzymatic treatment of mature municipal landfill leachate. Waste Manage 34, 798–803.
Kirk, T.K., Schultz, E., Connors, W., Lorenz, L., Zeikus, J., 1978. Influence of culture parameters on lignin metabolism by *Phanerochaete chrysosporium*. Arch. Microbiol. 117, 277–285.
Kulikowska, D., Klimiuk, E., 2008. The effect of landfill age on municipal leachate composition. Bioresour. Technol. 99, 5981–5985.
Kumar, V., Sharma, S.K., Sharma, T., Singh, V., 1999. Band gap determination in thick films from reflectance measurements. Opt. Mater 12, 115–119.
Kurniawan, T.A., Lo, W.H., Chan, G., 2006. Radicals-catalyzed oxidation reactions for degradation of recalcitrant compounds from landfill leachate. Chem. Eng. J. 125, 35–57.
Lata, H., Garg, V., Gupta, R., 2008. Adsorptive removal of basic dye by chemically activated ParthenCium biomass: equilibrium and kinetic modeling. Desalination 219, 250–261.
Lei, Y., Shen, Z., Huang, R., Wang, W., 2007. Treatment of landfill leachate by combined aged-refuse bioreactor and electro-oxidation. Water Res. 41, 2417–2426.
Li, G., Jiang, B., Li, X., Lian, Z., Xiao, S., Zhu, J., Zhang, D., Li, H., 2013. $C_{60}/Bi_2TiO_4F_2$ heterojunction photocatalysts with enhanced visible-light activity for environmental remediation. Acs Appl. Mater. Inter 5, 7190–7197.
Liu, J., Zhang, T., Wang, Z., Dawson, G., Chen, W., 2011. Simple pyrolysis of urea into graphitic carbon nitride with recyclable adsorption and photocatalytic activity. J. Mater. Chem. 21, 14398–14401.
Ozturk, I., Altinbas, M., Koyuncu, I., Arikan, O., Gomec-Yangin, C., 2003. Advanced physico-chemical treatment experiences on young municipal landfill leachates. Waste Manage 23, 441–446.
Pan, H., Zhang, Y.W., Shenoy, V.B., Gao, H., 2011. Ab initio study on a novel photocatalyst: functionalized graphitic carbon nitride nanotube. Acs Catal. 1, 99–104.
Pi, K., Gao, L., Fan, M., Gong, W., Wan, D., 2009. Two-stage biodegradation coupled with ultrafiltration for treatment of municipal landfill leachate. Process Saf. Environ. 87, 336–342.
Primo, O., Rivero, M.J., Ortiz, I., 2008. Photo-Fenton process as an efficient alternative to the treatment of landfill leachates. J. Hazard. Mater 153, 834–842.
Renou, S., Givaudan, J., Poulain, S., Dirassouyan, F., Moulin, P., 2008. Landfill leachate treatment: review and opportunity. J. Hazard. Mater 150, 468–493.
Rivas, F., Beltrán, F., Gimeno, O., Frades, J., Carvalho, F., 2006. Adsorption of landfill leachates onto activated carbon: equilibrium and kinetics. J. Hazard. Mater 131, 170–178.
Rodrıguez, J., Castrillon, L., Maranon, E., Sastre, H., Fernandez, E., 2004. Removal of non-biodegradable organic matter from landfill leachates by adsorption. Water Res. 38, 3297–3303.
Sanchis, S., Polo, A., Tobajas, M., Rodriguez, J., Mohedano, A., 2014. Coupling Fenton and biological oxidation for the removal of nitrochlorinated herbicides from water. Water Res. 49, 197–206.
Silva, T.F., Fonseca, A., Saraiva, I., Vilar, V.J., Boaventura, R.A., 2013. Biodegradability enhancement of a leachate after biological lagooning using a solar driven photo-Fenton reaction, and further combination with an activated sludge biological process, at pre-industrial scale. Water Res. 47, 3543–3557.
Tang, L., Zeng, G.M., Shen, G.L., Li, Y.P., Zhang, Y., Huang, D.L., 2008. Rapid detection of picloram in agricultural field samples using a disposable immunomembrane-based electrochemical sensor. Environ. Sci. Technol. 42, 1207–1212.
Vilar, V.J., Capelo, S.M., Silva, T.F., Boaventura, R.A., 2011a. Solar photo-Fenton as a pre-oxidation step for biological treatment of landfill leachate in a pilot plant with CPCs. Catal. Today 161, 228–234.
Vilar, V.J., Rocha, E.M., Mota, F.S., Fonseca, A., Saraiva, I., Boaventura, R.A., 2011b. Treatment of a sanitary landfill leachate using combined solar photo-Fenton and biological immobilized biomass reactor at a pilot scale. Water Res. 45, 2647–2658.
Wang, X., Maeda, K., Thomas, A., Takanabe, K., Xin, G., Carlsson, J.M., Domen, K., Antonietti, M., 2009. A metal-free polymeric photocatalyst for hydrogen production from water under visible light. Nat. Mater 8, 76–80.
Wang, Y., Shi, R., Lin, J., Zhu, Y., 2011. Enhancement of photocurrent and photocatalytic activity of ZnO hybridized with graphite-like C_3N_4. Energ Environ. Sci. 4, 2922–2929.
Xu, P., Zeng, G.M., Huang, D.L., Feng, C.L., Hu, S., Zhao, M.H., Lai, C., Wei, Z., Huang, C., Xie, G.X., Liu, Z.F., 2012. Use of iron oxide nanomaterials in wastewater treatment: a review. Sci. Total Environ. 424, 1–10.
Yan, S., Li, Z., Zou, Z., 2009. Photodegradation performance of g-C_3N_4 fabricated by directly heating melamine. Langmuir 25, 10397–10401.
Yang, C., Chen, H., Zeng, G., Yu, G., Luo, S., 2010. Biomass accumulation and control strategies in gas biofiltration. Biotechnol. Adv. 28, 531–540.
Zeng, G., Chen, M., Zeng, Z., 2013a. Risks of neonicotinoid pesticides. Science 340, 1403.
Zeng, G., Chen, M., Zeng, Z., 2013b. Shale gas: surface water also at risk. Nature 499, 154–154.
Zhang, C., Lai, C., Zeng, G., Huang, D., Yang, C., Wang, Y., Zhou, Y., Cheng, M., 2016. Efficacy of carbonaceous nanocomposites for sorbing ionizable antibiotic sulfamethazine from aqueous solution. Water Res. 95, 103–112.
Zhang, Q.Q., Tian, B.H., Zhang, X., Ghulam, A., Fang, C.R., He, R., 2013. Investigation on characteristics of leachate and concentrated leachate in three landfill leachate treatment plants. Waste Manage 33, 2277–2286.
Zhang, Y., Thomas, A., Antonietti, M., Wang, X., 2008. Activation of carbon nitride solids by protonation: morphology changes, enhanced ionic conductivity, and

photoconduction experiments. J. Am. Chem. Soc. 131, 50–51.
Zhang, Y., Zeng, G.M., Tang, L., Huang, D.L., Jiang, X.Y., Chen, Y.N., 2007. A hydroquinone biosensor using modified core–shell magnetic nanoparticles supported on carbon paste electrode. Biosens. Bioelectron. 22, 2121–2126.
Zhao, R., Novak, J.T., Goldsmith, C.D., 2012. Evaluation of on-site biological treatment for landfill leachates and its impact: a size distribution study. Water Res. 46, 3837–3848.
Zhou, S., Liu, Y., Li, J., Wang, Y., Jiang, G., Zhao, Z., Wang, D., Duan, A., Liu, J., Wei, Y., 2014. Facile in situ synthesis of graphitic carbon nitride (g-C3N4)-N-TiO2 heterojunction as an efficient photocatalyst for the selective photoreduction of CO2 to CO. Appl. Catal. B Environ. 158, 20–29.